ORGANOMETALLICS

pubs.acs.org/Organometallics Article

ToF-SIMS Investigation of the Initial Stages of MeCpPt(CH_3)$_3$ Adsorption and Decomposition on Nickel Oxide Surfaces: Exploring the Role and Location of the Ligands

Mahsa Konh, Clinton Lien, Xuefen Cai, Su-Huai Wei, Anderson Janotti, Francisco Zaera, and Andrew V. Teplyakov*

Cite This: *Organometallics* 2020, 39, 1024−1034 Read Online

ACCESS | Metrics & More | Article Recommendations | Supporting Information

ABSTRACT: The chemistry of trimethyl(methylcyclopentadienyl)platinum(IV) (MeCpPt(CH_3)$_3$), a platinum organometallic compound often used for the chemical deposition of Pt films, on nickel oxide surfaces was investigated. Particular emphasis was placed on following the coordination of the initial ligands, methylcyclopentadienyl (MeCp) and methyl moieties, by using time-of-flight secondary ion mass spectrometry (ToF-SIMS) in combination with X-ray photoelectron spectroscopy (XPS) and density functional theory (DFT) computations. It is shown that the MeCp fragment is stable and, upon reacting with NiO surface, remains attached to the Pt center. The methyl groups, on the other hand, can migrate to the nickel surface or remain bonded to the Pt, but on NiO surfaces they prefer to interact with the nickel centers rather than with the oxygen atoms. In addition to these findings, ToF-SIMS data confirmed that gas-phase electron-impact activation can truly enhance the activity of the MeCpPt-(CH_3)$_3$ precursor.

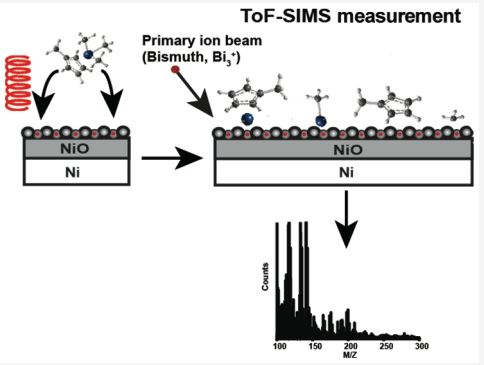

INTRODUCTION

The use of organometallic compounds spans a vast landscape of applications, largely relying on the nature of the interaction of the metal atom with the corresponding ligands. One of the fields that marries the chemical reactivity of organometallic compounds and their ability to deliver a metallic center to a support material is heterogeneous catalysis.[1−8] Within this field, platinum-containing organometallics have been considered as a way of both delivering the platinum metal to control the formation of nanoparticles of specific sizes on support materials in chemical vapor deposition (CVD) and atomic layer deposition (ALD) processes[9−12] and designing specific single atom catalytic centers, whose reactivity and selectivity are determined by the appropriate ligands.[13] Ligands such as diketonates, amidinates, or cyclopentadienyls have been frequently used in this type of surface applications.

Despite the exceptional reactivity and selectivity of platinum-based catalysts, the high cost of this metal has prompted a number of attempts to dilute it within alloy compounds or place single platinum atoms or small nanoparticles with high precision on relatively cheap substrates. The chemistry of Pt-containing organometallic precursors is key in both of these approaches, since methods such as ALD allow for the atomically controlled design of metal-containing surface features.[14,15] However, full optimization of such depositions requires complete understanding of the energy landscape of the process. One of the issues with Pt precursors is that only a few of them possess the high volatility required for clean evaporation, and those normally are relatively unreactive, meaning that either thermal activation or electron-impact activation is required to initiate the surface chemistry that ultimately leads to metal deposition.[16] In that regard, it is crucial to understand the fate of the ligands of the target platinum organometallic precursor; that may define the chemical state of platinum, the size distribution of the deposited nanoparticles (or properties of films), the nature of the interface (or intermixing) of the platinum and the other metals, and ultimately the catalytic activity of the catalysts made this way.

Among the transition metals used in combination with platinum, nickel has a very special place. Pt−Ni alloys are promising candidates for many catalytic and electrocatalytic processes.[8] The role of nickel is often to weaken the otherwise very strong interaction of Pt with reactants or products such as CO that poison the catalysts.[2] At the same time, NiO has been shown to be an essential part of photocatalysts used to produce molecular hydrogen in hydrogen fuel cells. In 2014 Zaera et al. described a model in which protons are reduced on

Special Issue: Organometallic Chemistry at Various Length Scales

Received: November 15, 2019
Published: February 3, 2020

https://dx.doi.org/10.1021/acs.organomet.9b00781
Organometallics 2020, 39, 1024−1034

Scheme 1. Proposed Reaction Pathways for the $MeCpPt(CH_3)_3$ Deposition Precursor on NiO Substrates via Gas-Phase Electron-Impact and Thermal Activation

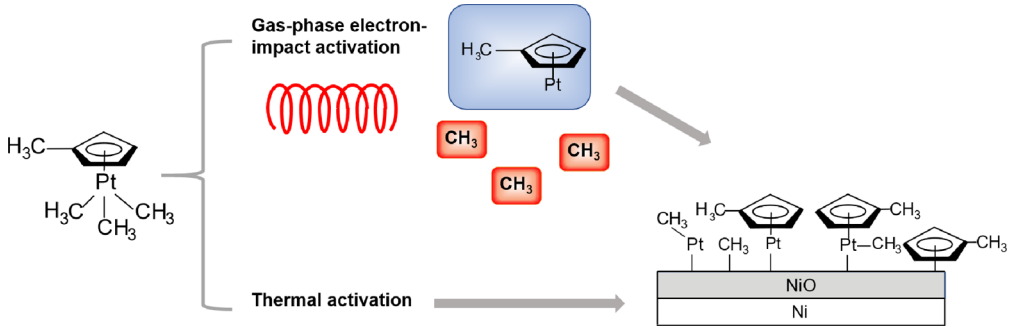

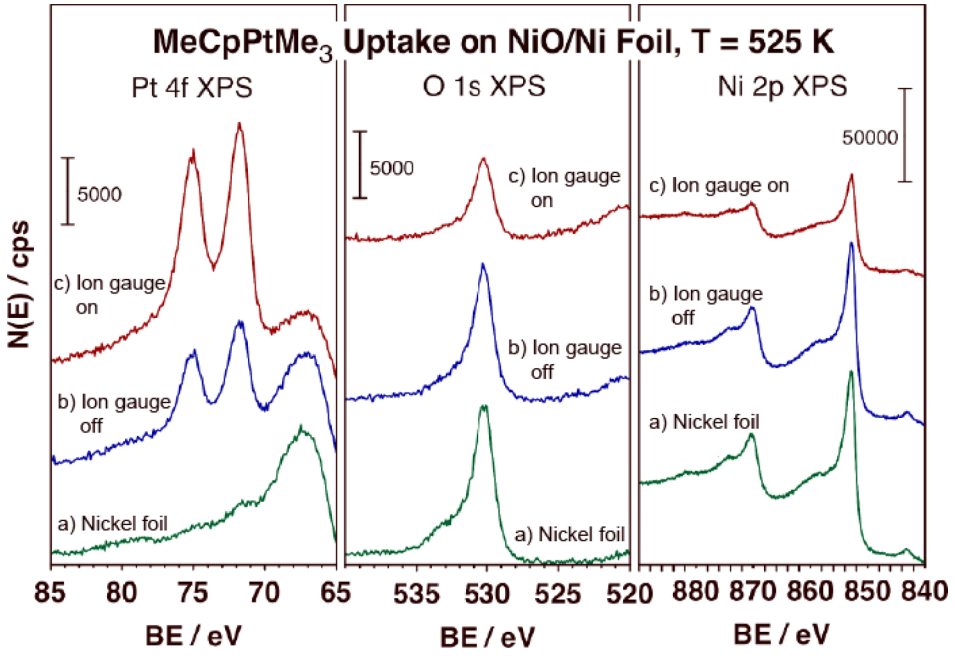

Figure 1. Summary of the XPS investigation of platinum deposition on NiO using $MeCpPt(CH_3)_3$. The figure compares three spectroscopic regions, corresponding to the Pt 4f, O 1s, and Ni 2p photoelectrons, for (a) a clean surface, (b) the same surface as (a) exposed to 1×10^6 L of $MeCpPt(CH_3)_3$ with the ion gauge off, and (c) after a 5×10^5 L dose of the same precursor with the ion gauge on. The temperature of the surface during deposition was 525 K.

semiconductor surfaces but require the recombination of the resulting hydrogen atoms on a metal surface to produce hydrogen molecules.[17] It has also been shown that the combination of a NiO support with metallic nanoparticles can be efficient for the promotion of photocatalysis in methanol fuel cells.[18] Thus, the deposition of platinum in a controlled manner onto NiO surfaces promises to lead to the formation of an exceptional catalytic material. In order to exert the required deposition control, the mechanism of platinum deposition on NiO surfaces requires atomic level understanding.

The deposition of Pt by ALD commonly comprises two half reactions, following a process initially introduced in 2003 by Aaltonen et al.[12] The first half-reaction delivers the organometallic Pt precursor to the surface, and the second uses exposure to O_2 gas to remove the carbon-containing byproducts. This approach allows precise control of the amount of platinum introduced to the support material. Over the years, trimethyl(methylcyclopentadienyl)platinum(IV) ($MeCpPt(CH_3)_3$) has been the most commonly used platinum deposition precursor.[19−25] Detailed investigations of the deposition mechanism of Pt have used this precursor to evaluate every step of the process;[24,26−28] however, it has been found that the stability of $MeCpPt(CH_3)_3$ presents a number of challenges associated with its initial activation as well as with the complete removal of the ligands from the surface.[24,25,29−33] It has been recently shown by us that gas-phase electron-impact activation of $MeCpPt(CH_3)_3$ results in an increase uptake of Pt on silicon oxide surfaces, also leaving behind cleaner surfaces with less carbon contamination than those obtained following thermal methods (Scheme 1).[16,34] X-ray photoelectron spectroscopy (XPS) investigations provided carbon-to-Pt ratios consistent with the MeCp fragment being bound to Pt and with most methyl groups being eliminated from the precursor upon deposition. Additional time-of-flight secondary ion mass spectrometry (ToF-SIMS) studies confirmed this hypothesis and identified the organic species that form on the substrate as MeCp bound to Pt together with additional isolated methyl groups. These observations were found to be consistent with the independent determination, by

https://dx.doi.org/10.1021/acs.organomet.9b00781
Organometallics 2020, 39, 1024−1034

mass spectrometry, that gas-phase electron-impact ionization leads to the removal of one or more methyl groups from $MeCpPt(CH_3)_3$.[35]

Extension of this approach to evaluate the adsorption and reactions of this Pt deposition precursor molecule on NiO surfaces brings about a number of additional challenges. In particular, the presence of two different metallic sites may affect the final binding of the ligands and may be susceptible to ligand migration. Specifically, it is important to determine the preferred final adsorption site of the MeCp fragment, whether on the original Pt metal center or on a surface site within the support material on Ni or O atoms. It is also important to determine if electron-impact activation affects the distribution of methyl groups on the surface bound to nickel, platinum, or oxygen.

In order to address these issues, we have recently introduced the use of ToF-SIMS, a technique that offers high mass resolution and allows to extract intricate details of specific species bound to a surface. This extremely sensitive analytical technique is commonly applied to characterize thin films;[36−40] in a previous investigation, we also confirmed that ToF-SIMS is a precise technique that can be utilized to identify the nature of surface moieties produced by chemical reactions on surfaces such as the ones occurring in ALD processes.[34]

Here, we report on the adsorption and decomposition of $MeCpPt(CH_3)_3$ on NiO. We follow the formation and binding of surface species produced by thermal reaction and by gas-phase electron-impact activation, and we trace the fate of the organic ligands produced on the surface. This work paves the way for the design of deposition processes with controlled platinum deposition on metal oxides, and also helps understand the rules governing the formation of multicomponent nanoparticles and thin films based on the surface chemistry of organometallic precursors.

RESULTS AND DISCUSSION

The experimental studies combine deposition and initial characterization with XPS at the University of California, Riverside, and ToF-SIMS investigations at the University of Delaware. The details of the sample preparation and transfer are described below in the Experimental and Computational Section.

In order to identify the interface chemistry during the initial steps of platinum deposition onto NiO or for the first half-cycle of Pt ALD onto this material, it is important to understand the nature of the possible species present on a surface in a thermal process as opposed to that resulting from a gas-phase electron-impact ionization protocol.

Figure 1 summarizes the results from the XPS characterization of the samples performed at UC Riverside before they were shipped to the University of Delaware. The presence of platinum deposited under both thermal and electron-impact ionization conditions (with ion gauge on) is clearly observed. The measured binding energy (BE) for the Pt $4f_{7/2}$ peak is 71.3 eV, indicating a slight positive charge on the Pt center; the reported value for metallic Pt is BE = 70.9 eV.[41] This is not surprising given the binding to a more electronegative NiO surface; a similar shift was seen on SiO_2.[16] This deposition appears not to affect the state of the surface oxygen or nickel in any substantial way. The peak below 70 eV in the Pt 4f spectral region corresponds to Ni 3p, as supported by the presence of the same peak in the spectrum of a clean NiO surface. The O 1s peak is centered at BE = 529.8 eV, a value typical of NiO, and the Ni $2p_{3/2}$ spectra show a dominant peak at BE = 852.3 eV, for metallic nickel, slightly broadened in the high BE side by a small signal originating from a NiO thin film (as mentioned in the Experimental and Computational Section). The only noticeable change seen in the spectra upon adsorption of the Pt precursor is an intensity decrease in both O 1s and Ni 2p signals. That decrease is larger in the data for the deposition experiments with the ion gauge on, consistent with the higher amount of platinum deposited, which was estimated (based on a signal intensity calibration from previous experiments) to be approximately half the monolayer for the thermal deposition and approximately one monolayer for the experiments with ion gauge on.[21] Clearly, the gas-phase electron-impact excitation of the precursor enhances deposition, as twice the Pt coverage was obtained this way with only half of the dose. Also, on the basis of our past studies, the carbon-to-platinum ratios of the adsorbed species in both sets of conditions was estimated here to be about 6 to 1 or less, consistent with the MeCp fragment remaining attached to the adsorbed Pt atoms.

Upon transfer of the samples to the University of Delaware, and before carrying out their ToF-SIMS characterization, any possible changes in the morphology of the NiO foil were checked with atomic force microscopy (AFM). No noticeable changes were recorded for any of the three samples (see Figure S1 in Supporting Information section).

Information about the amount, type, or binding site of the methyl or MeCp ligands on these samples was then extracted from the additional ToF-SIMS data acquired in this study. On the basis of our previous work,[16,34] the expectation of the effect of gas-phase electron-impact activation during the dosing of the Pt precursor is not only to enhance its uptake, as already determined by XPS, but also to reduce the amount of organic species deposited, as the intermediates formed in the gas phase are presumed to have undergone removal of all (or most) of the methyl groups attached directly to the Pt center of the molecule. The ToF-SIMS spectra shown below for each region of interest compare data for the same three samples described on Figure 1: the clean NiO sample, the same surface exposed to 1×10^6 L of $MeCpPt(CH_3)_3$ with the ion gauge off, and the surface after a 5×10^5 L exposure to the same precursor with the ion gauge on.

As shown in Figure 2, the methylcyclopentadienyl (MeCp) fragment, recorded as the major peak, is intact on the two surfaces dosed with the precursor. Although the presence of a

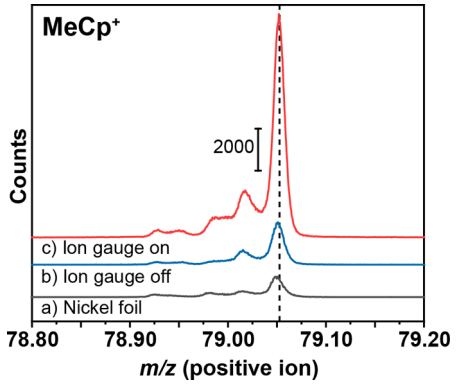

Figure 2. High resolution ToF-SIMS spectral region corresponding to the MeCp fragment on (a) clean surface, the same surface as (a) exposed to $MeCpPt(CH_3)_3$ with the ion gauge (b) off, and (c) on.

https://dx.doi.org/10.1021/acs.organomet.9b00781
Organometallics 2020, 39, 1024−1034

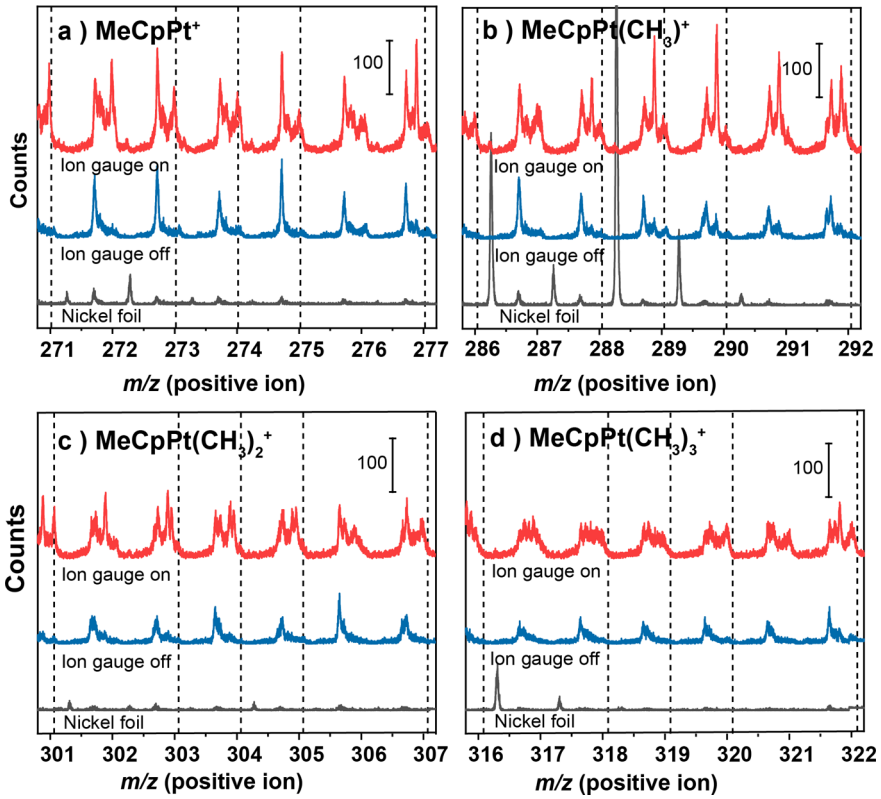

Figure 3. (Color online) High resolution ToF-SIMS spectral regions corresponding to all the possible $MeCpPt(CH_3)_x$ fragments ($x = 0-3$) for the samples prepared having the ion gauge on (red) and off (blue) and on a blank nickel foil (black): (a) MeCpPt, (b) $MeCpPt(CH_3)$, (c) $MeCpPt(CH_3)_2$, (d) $MeCpPt(CH_3)_3$. The expected positions of the peaks corresponding to the indicated fragments (with different Pt isotopes, $^{192}Pt/^{194}Pt/^{195}Pt/^{196}Pt/^{198}Pt$) are shown by the dotted lines.

small amount of C6 hydrocarbons with the same mass-to-charge ratio is also identified on a clean nickel foil sample, the intensity of that feature increases dramatically for the sample exposed to $MeCpPt(CH_3)_3$, especially with the ion gauge on. Overall, this set of measurements is consistent with MeCp fragments being present on the surface following Pt deposition. This observation also suggests that the surfaces investigated are largely unaffected by the conditions endured during transportation. Moreover, although these ToF-SIMS results can only be treated as semiquantitative, it is clear that the intensity of the $MeCp^+$ peak increases by more than an order of magnitude upon exposure of the surface to the Pt precursor with the ion gauge on; the presence of this fragment on a surface following deposition is beyond doubt.

In analogy with our previous investigations of Pt ALD on silica samples using the same precursor, the MeCp fragment is likely to be bound to the Pt atom on the NiO surface as well. In order to confirm the nature of the surface species in this study, the ToF-SIMS measurements of the molecular fragments with overall formulas of $MeCpPt(CH_3)_x$ are summarized in Figure 3. These fragments are expected to be the main chemical moieties formed upon adsorption, since MeCp ligands are stable and the energy barrier required to remove MeCp from metallic Pt is quite high; only strong oxidants such as ozone or oxygen plasma[42,43] are capable to remove them in ALD processes. Nevertheless, it is important to obtain direct experimental evidence for the presence of such species on the surface. Taking into account the known ratios of the stable isotopes of Pt ($^{192}Pt:^{194}Pt:^{195}Pt:^{196}Pt:^{198}Pt$ = 1:33:34:25:7), the results in Figure 3 clearly show that surface fragments containing both Pt and the MeCp ligand are indeed present on the surface. Furthermore, careful comparison of the results in panels a through d in Figure 3 suggests that MeCpPt, and to the lesser extent $MeCpPt(CH_3)$, are the most abundant fragments on these surfaces; no $MeCpPt(CH_3)_2$ or $MeCpPt(CH_3)_3$ are detectable within the experimental errors of our instrument. This summary also confirms that deposition with the ion gauge on is much more efficient than with the ion gauge off, and that none of these fragments are present on the blank sample, where the nickel surface was not exposed to $MeCpPt(CH_3)_3$.

Thus, Figure 3a indicates that MeCpPt is the major Pt-containing fragment on the surface. The next question relates to the fate of the methyl ligands. It is expected that, under the conditions of the deposition, at least a fraction of methyl groups bound to the adsorbed platinum atoms or to the nickel surface may undergo thermal transformation (hydrogenation, dehydrogenation, carbon−carbon coupling) and become removed from the surface. This assumption is fully consistent with the previous studies of methyl groups on platinum single crystal surfaces.[44−48] Nevertheless, some methyl groups, from surface thermal decomposition or directly originating from the gas-phase decomposition of the precursor, may still attach directly to the NiO surface. To explore this possibility, the ToF-SIMS spectral regions corresponding to the fragments with $Ni(CH_3)_x$ and $NiO(CH_3)_x$ overall formula were interrogated. In Figure 4, parts a, b, and c show the regions corresponding to m/z of $Ni(CH_3)^+$, $Ni(CH_3)_2^+$, and $Ni(CH_3)_3^+$ and panels d, e, and f summarize the regions corresponding to m/z of $NiO(CH_3)^+$, $NiO(CH_3)_2^+$, and

https://dx.doi.org/10.1021/acs.organomet.9b00781
Organometallics 2020, 39, 1024−1034

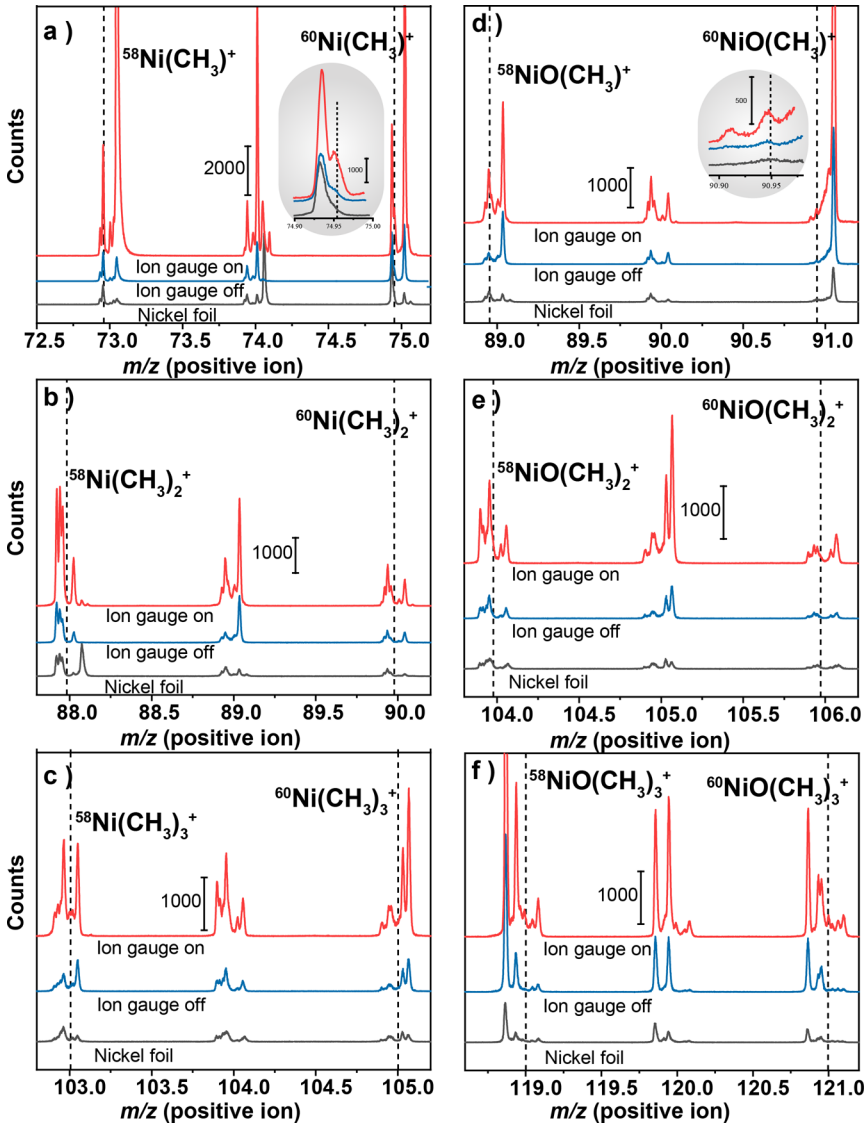

Figure 4. (Color online) High resolution ToF-SIMS spectral regions corresponding to all possible $Ni(CH_3)_x$ and $NiO(CH_3)_x$ fragments for the samples prepared having the ion gauge on (red) and off (blue) and on the blank nickel foil (black) indicated (a) $Ni(CH_3)$ (with an inset showing $^{60}Ni(CH_3)^+$ species), (b) $Ni(CH_3)_2$, (c) $Ni(CH_3)_3$, (d) $NiO(CH_3)$ (with an inset showing $^{60}NiO(CH_3)^+$ species), (e) $NiO(CH_3)_2$, (f) $NiO(CH_3)_3$. The expected positions of the peaks corresponding to these fragments (with two major Ni isotopes, $^{58}Ni/^{60}Ni$) are shown by the dotted lines.

$NiO(CH_3)_3^+$, respectively. The $Ni(CH_3)$ and $NiO(CH_3)$ peaks are indeed clearly observed, as confirmed by the isotopic ratio of two major stable isotopes of Ni (^{58}Ni:^{60}Ni = 68:26). However, there is no clear confirmation of any surface species containing nickel and more than one methyl group. This is an important observation, because although it would be unlikely for thermal chemistry to produce surface Ni-containing species with more than one methyl group, exposure to higher fluxes of methyl radicals from the electron-impact ionization process could potentially lead to the formation of surface species with higher coordinations of adsorbates. It should be noted that a very small amount of $Ni(CH_3)$ and $NiO(CH_3)$ species are presented on a clean surface that is not exposed to the platinum precursor; however, the amount of the recorded signal is much smaller than for the exposed samples. Nevertheless, this observation is a warning that some adventitious carbon fragments could affect the attempts to quantify these ToF-SIMS results. That said, the zoom-in portions of $^{60}Ni(CH_3)^+$ and $^{60}NiO(CH_3)^+$ spectral regions provide a very important glimpse into the surface ligand placement for methyl groups on NiO surface. Although both types of species are observed, the intensity corresponding to the $^{60}Ni(CH_3)^+$ fragment, consistent with the methyl group bound directly to the Ni site, is at least an order of magnitude higher than that of the $^{60}NiO(CH_3)^+$ fragment. Assuming that the ionization cross sections for both species are similar, this result shows that the majority of methyl groups on NiO surface are bound directly to the Ni site and not form a methoxy species at the conditions of this experiment. It should also be noted that the $^{60}NiO(CH_3)^+$ fragment could indeed indicate the presence of a methoxy group bound to a nickel site, but also could simply show the presence of an O = $^{60}Ni(CH_3)^+$ species, with the methyl group still coordinated directly to a nickel (not oxygen) atom. This conclusion that the methyl moieties are primarily coordinated to Ni is fully supported by the computational studies discussed below.

https://dx.doi.org/10.1021/acs.organomet.9b00781
Organometallics 2020, 39, 1024−1034

The possibility of the formation of $Pt(CH_3)_x$ surface species was also investigated. According to the results provided above in Figure 3, MeCp ligands certainly bind to Pt-containing fragments on the surface following Pt precursor exposure. According to Figure 5, despite the semiquantitative nature of

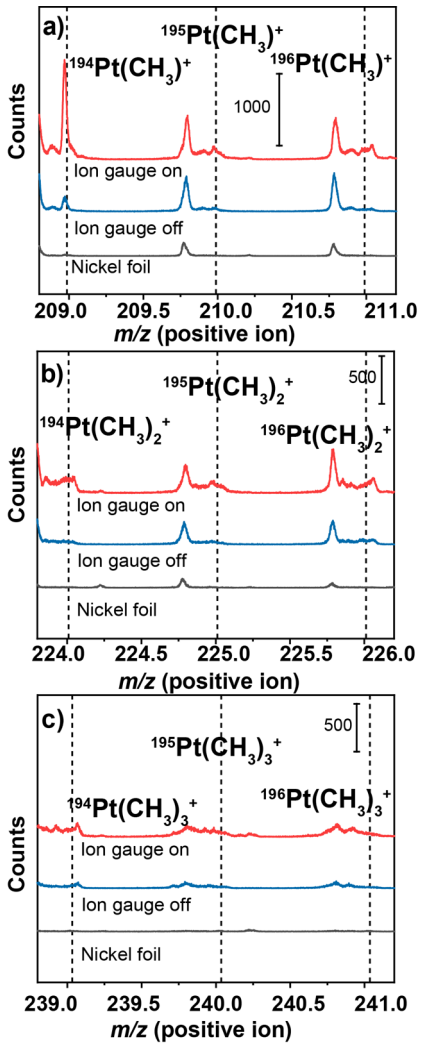

Figure 5. (Color online) High resolution ToF-SIMS spectral regions corresponding to all possible $Pt(CH_3)_x$ fragments for the samples prepared having the ion gauge on (red) and off (blue) and on the blank nickel foil (black) indicated (a) $Pt(CH_3)$, (b) $Pt(CH_3)_2$, (c) $Pt(CH_3)_3$. The expected positions of the peaks corresponding to these fragments (with three major Pt isotopes, $^{194}Pt/^{195}Pt/^{196}Pt$) are shown by the dotted lines.

ToF-SIMS, some $Pt(CH_3)$ moieties appear to be detected on the surface (Figure 5a). The presence of significant amounts of $Pt(CH_3)_2$ and $Pt(CH_3)_3$ fragments can be ruled out (Figures 5b and 5c, respectively). Although the formation of the $Pt(CH_3)$ fragments is difficult to quantify, especially since they may simply be the result of decomposition of the $MeCpPt(CH_3)$ adsorbed species, the intensity of the peak corresponding to the $Pt(CH_3)$ species in a sample exposed to the $MeCpPt(CH_3)_3$ with the ion gauge on is higher than that detected with the other surfaces, perhaps because of a combination of more efficient deposition and a possible deposition of gas-phase methyl radicals produced during electron impact ionization of the Pt precursor.

Finally, it is also important to probe the possibility that the MeCp ligand may bind directly to the Ni surface. Figure 6 explores this pathway by focusing on the regions corresponding to $MeCpNi(CH_3)_x$ ions. Unfortunately, this m/z region is so crowded that it is very difficult to confirm the existence of such species or to rule out their formation.

Overall, the results of the ToF-SIMS investigation are consistent with our preliminary XPS assignment. The formation of MeCpPt and $MeCpPt(CH_3)$ species on the NiO surface was confirmed. The formation of adsorbed $Ni(CH_3)$ species (and possibly a very small amount of methoxy groups) was also observed. As expected, gas-phase electron-impact ionization increases the efficiency of the Pt deposition in a noticeable way, by almost an order of magnitude in some cases, and possibly provides additional methyl radicals that can interact with the surface, attaching to both Ni and Pt sites.

Some further information can be extracted from our data if complemented by quantum mechanics calculations of the strength of bonding of MeCp and methyl fragments to the metal center and to the NiO surface. First, the bond strength of methyl and methylcyclopentadienyl groups to the metal centers were explored by DFT calculations, for platinum and for nickel. The three reference compounds investigated with this approach were $MeCpPt(CH_3)_3$, $(MeCp)_2Ni$, and $C_5H_5Ni(PPh_3)(CH_3)$. The strengths of the relevant bonds were estimated by optimizing the initial structure, removing a methyl or a MeCp group, and reoptimizing the final structures. The results of this work are summarized in Table 1. The strength of methyl-Pt bond in $MeCpPt(CH_3)_3$ was calculated to be −191.5 kJ/mol, which is about 40 kJ/mol stronger than the methyl-Ni bond in the comparison reaction. It appears that if methyl groups produced via electron-impact ionization would attach to platinum atoms, their removal at the temperature of the experiment is unlikely. Also, compared to the methyl group, the MeCp entity is bound much more strongly to both metals, with predicted bond strengths of −218.5 kJ/mol and −208.0 kJ/mol on platinum and nickel, respectively. These initial predictions are fully consistent with the assumption that the MeCp group is very unlikely to detach from the platinum atom if MeCpPt is formed on the surface of the support material.

To reinforce the conclusions reached by this simple exercise, a bonding energy comparison can also be made with methyl versus C_5H_5 (Cp) groups on single-crystal surfaces of Pt and Ni. According to previous reported studies, summarized in Table 2, methyl groups are stable on both Pt(111) and Ni(100) surfaces, having high adsorption energies. Methyl groups on platinum are more stable than on nickel, by about 35 kJ/mol.[49,50] In addition, aromatic rings, in this case the Cp ring, show greater stability than alkyl groups on both metal surfaces; the binding energy of Cp, at around 270 kJ/mol on both metals, is at least 50 kJ/mol larger than that of the methyl group.[51,52] This result is also consistent with the ToF-SIMS data showing that MeCp is strongly bonded to platinum, and suggests that it is not likely for it to migrate to the NiO surface.

Finally, can computational studies help us understand the chemical transformations that methyl and MeCp groups may undergo on the actual NiO surface? First, we determined the most stable position for a Pt adatom on the NiO(001), and then studied the interaction between the Pt adatom and a corresponding ligand (methyl or methylcyclopentadienyl). To evaluate the stability of the surface species, we calculated the

https://dx.doi.org/10.1021/acs.organomet.9b00781
Organometallics 2020, 39, 1024−1034

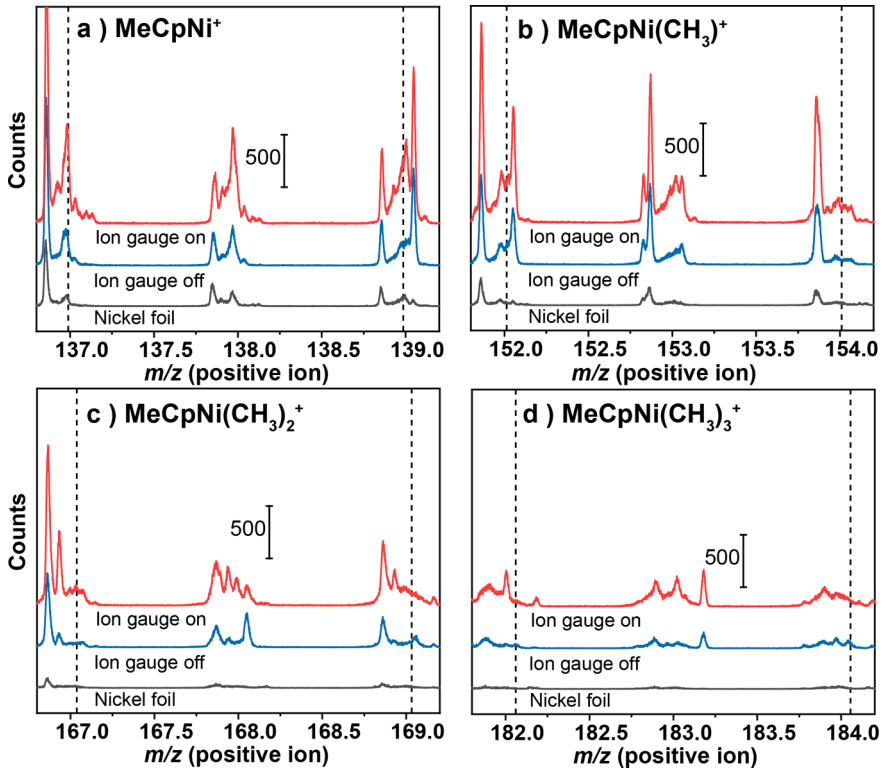

Figure 6. (Color online) High resolution ToF-SIMS spectral regions corresponding to the possible $MeCpNi(CH_3)_x$ fragments for the samples with ion gauge on (red) and off (blue) and on the blank nickel foil (black) indicated: (a) MeCpNi, (b) $MeCpNi(CH_3)$, (c) $MeCpNi(CH_3)_2$, (d) $MeCpNi(CH_3)_3$. The expected positions of the peaks corresponding to these fragments (with two major Ni isotopes, $^{58}Ni/^{60}Ni$) are shown by the dotted lines.

Table 1. Bond Strength Comparison for Methyl and MeCp Group Attached to Pt or Ni within Model Organometallic Compounds

reaction investigated	bond energy predicted for the reactions indicated, kJ/mol
$MeCpPt(CH_3)_3 = MeCpPt(CH_3)_2 + CH_3$	−191.5
$C_5H_5Ni(PPh_3)(CH_3) = C_5H_5Ni(PPh_3) + CH_3$	−151.6
$MeCpPt(CH_3)_3 = Pt(CH_3)_3 + MeCp$	−218.5
$(MeCp)_2Ni = NiMeCp + MeCp$	−208.0

Table 2. Adsorption Energy Comparison for Methyl versus Cyclopentadienyl on Pt(111) Versus Ni(100) Surfaces

	adsorption energy, kJ/mol
Methyl on Ni(100)[49]	−192
Methyl on Pt(111)[50]	−225
C_5H_5 on Ni(100)[51]	−273
C_5H_5 on Pt(111)[52]	−279

difference in energy between the species adsorbed on Pt adatom and on NiO by using eq 1

$$E_b = E(\text{NiO:Pt} + X) + E(\text{NiO}) - E(\text{NiO:Pt}) - E(\text{NiO:}X) \quad (1)$$

where X represents the methyl or MeCp ligands, $E(\text{NiO:Pt} + X)$ is the total energy of the NiO(001) surface containing a Pt adatom and the X ligand, $E(\text{NiO})$ is the total energy of the bare NiO(001) surface, and $E(\text{NiO:Pt})$ and $E(\text{NiO:}X)$ are the total energies of the most stable configurations of NiO(001) containing a Pt adatom and NiO(001) containing with the X ligand, respectively. With such a definition, $E_b < 0$ indicates that the adsorption process is exothermic; that is, the formation of the $E(\text{NiO:Pt} + X)$ system is energetically favorable.

The first observation derived from these calculations is that a methyl group prefers to be bonded to a Pt adatom on a model NiO(001) surface, as shown in Figure 7c; this is much more stable, by about 166 kJ/mol, than the methyl group being attached to Ni on the NiO(001) surface (Figure 7b), and 230 kJ/mol more stable than when the methyl group is attached to O (Figure 7a); i.e., without the Pt adatom, the most stable configuration corresponds to the methyl group bonded directly to a nickel atom, with a bond length of 1.96 Å, as opposed to bonding to an oxygen atom of the same surface. This result is in a full agreement with the ToF-SIMS data showing that the majority of the methyl groups on NiO are bound directly to the Ni site. In addition, the stability of MeCp group was investigated in three positions; on platinum adatom, and on either nickel or oxygen atoms on the surface, as shown in Figure 7d–f. The results showed clearly that adsorption of MeCp on platinum adatom is much more stable, by about 239 kJ/mol, than MeCp adsorption on the nickel or by 252 kJ/mol on oxygen sites of the NiO surface. This can be related to the partial positive charge on platinum that interacts strongly with the cyclopentadienyl ring. This conclusion also fully supports the ToF-SIMS observation of MeCpPt being the major adsorbate in these studies.

https://dx.doi.org/10.1021/acs.organomet.9b00781
Organometallics 2020, 39, 1024−1034

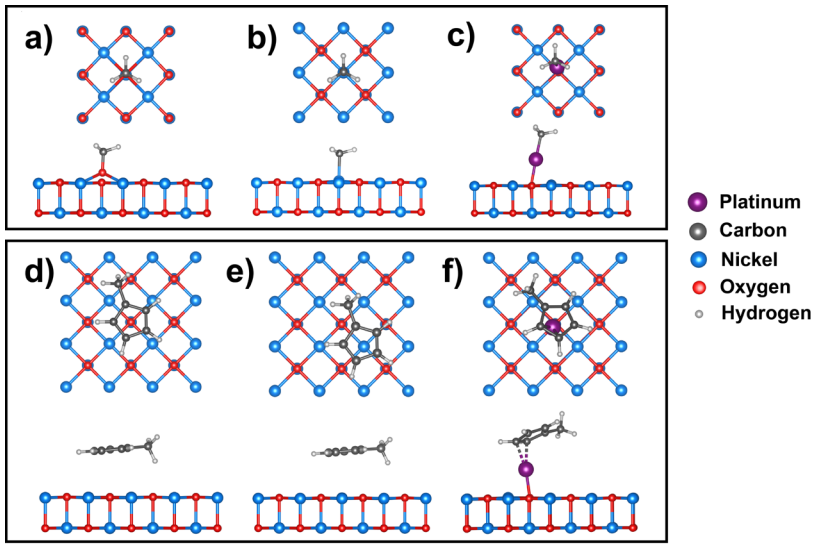

Figure 7. Molecular arrangement of methyl and methylcyclopentadienyl groups on NiO surface. Methyl on (a) oxygen atom, (b) nickel atom, (c) platinum adatom, and methylcyclopentadienyl group on (d) oxygen atom, (e) nickel atom, and (f) platinum adatom.

CONCLUSIONS

In this work we have explored the initial stages of platinum deposition using $MeCpPt(CH_3)_3$ onto NiO surfaces by combining XPS and ToF-SIMS experimental work with computational predictions. XPS data suggested that both thermal and electron-impact stimulated adsorption of the platinum precursor lead largely to the formation of surface species with an overall carbon-to-platinum ratio of approximately 6, consistent with the retention of MeCp surface species, likely still coordinated to the Pt center. An enhancement in Pt XPS signal also indicated that electron-impact activation of the precursor in the gas phase makes the deposition process much more efficient. In order to understand which surface species are actually formed, ToF-SIMS investigations were carried out, focusing on the spectral regions corresponding to the most likely Ni- and Pt-containing surface species. The existence of MeCpPt and $MeCpPt(CH_3)$ surface moieties, and their dominant role in the deposition chemistry, was confirmed, as was the formation of Ni−C bonds in $Ni(CH_3)$ (or $NiO(CH_3)$) fragments. These findings are fully consistent with the previously confirmed formation of MeCpPt species as the main fragments formed by electron-impact ionization of $MeCpPt(CH_3)_3$ in the gas phase, established via the use of mass spectrometry. The possibility of surface migration of the MeCp and methyl ligands was evaluated via computational work, which led to the conclusions that the thermal chemistry of the adsorbed intermediates generates mostly MeCp fragments attached to Pt atoms and that methyl group bound directly to a Ni site is the most stable configuration for methyl interaction with NiO. Further work would be necessary to fully understand the deposition process for Pt onto transition metal oxides; however, this work provides an important starting point for such analysis.

EXPERIMENTAL AND COMPUTATIONAL SECTION

The deposition of Pt on nickel foils using the $MeCpPt(CH_3)_3$ precursor, as well as the XPS characterization of the resulting samples, were performed in a two-tier stainless-steel ultrahigh vacuum (UHV) apparatus described in previous publications.[21,53,54] The nickel foil used as the substrate was purchased from Sigma-Aldrich (99.995% purity), initially cleaned by immersing it in a diluted HF solution (deionized water:HF = 1:20), mounted on the rod used for the transfer of samples between the two chambers, and lightly sputtered and annealed before each adsorption experiment. Initial XPS characterization of these films indicated the persistence of a thin (∼1 nm thick) NiO film on top of the metallic Ni. The temperature of the surface was monitored using a K-type thermocouple inserted between the sample and the metallic clip that holds the sample in place. An ionization gauge is coupled to the UHV system for two purposes, to monitor the pressure of the gases during dosing and as a gas-phase electron-impact activating source for the organometallic Pt compound, as we have discussed before.[16,55] The $MeCpPt(CH_3)_3$ precursor (purchased from Sigma-Aldrich 98% purity) was purified in situ via repeated freeze−pump−thaw cycles before introduction to the side chamber for surface dosing. This auxiliary chamber has a base pressure of 1×10^{-8} Torr, maintained by using a turbomolecular pump. A pressure of $P_{exposure} = 5 \times 10^{-5}$ Torr was used for the Pt precursor dosing, carried out for 5 h (amounting to a total dose of $\sim 1 \times 10^6$ L) for the case of thermal adsorption (ion gauge off), and a 6×10^{-5} Torr exposure for 2.5 h (equivalent to $\sim 5 \times 10^5$ L) was used for the case where the ion gauge was kept on (for electron-impact activation). Adsorption of the Pt precursor was carried out at a substrate temperature of 525 K. More details of the dosing procedure have been published elsewhere.[21] After deposition, the samples were transferred to the main chamber, which is kept at a base pressure of 5×10^{-10} Torr, for characterization by XPS. The XPS data were acquired using the Kα emission of the aluminum anode ($h\upsilon$ = 1486.6 eV) of a non-monochromatized dual Mg−Kα/Al−Kα X-ray excitation source, with its natural line width (0.85 eV), and a Leybold EA11 hemispherical electron energy analyzer equipped with a multichannel detector. All binding energies were referred to a value of BE = 852.3 eV for the Ni $2p_{3/2}$ peak of the metallic substrate.[41] No further processing of the data was carried out: the spectra reported in Figure 1 are the raw data, only displaced in the y direction to facilitate viewing.

ToF-SIMS experiments were performed using a ToF-SIMS instrument (ToF-SIMS IV, ION-TOF, Münster, Germany). A 25 keV monoisotopic Bi_3^+ ion beam was used to obtain static negative and positive SIM spectra. The illustrated data are the result of 50 scans added up collected with a mass resolution of $m/\Delta m$ = 9000 over an area of analysis of 500 × 500 μm^2 at room temperature. Typical ion fluences of 1×10^{12} ions/cm^2 were used to make sure that no substantial sputtering of the surface takes place. On the basis of the nature of the substrate and the precursor, only positive ion spectra are shown in this paper; however, both positive- and negative-ion spectra were collected. The masses used for calibration were those for the H^+,

https://dx.doi.org/10.1021/acs.organomet.9b00781
Organometallics 2020, 39, 1024−1034

H_2^+, H_3^+, C^+, CH^+, CH_2^+, CH_3^+, $C_2H_3^+$, $C_3H_5^+$, $C_4H_7^+$, $C_5H_5^+$, $C_6H_5^+$, $C_7H_7^+$, and Pt^+ ions in positive mode and for the H^-, H_2^-, C^-, CH^-, CH_2^-, CH_3^-, C_2^-, C_2H^-, C_3^-, C_4^-, C_5^-, C_6^-, and C_7^- ions in negative mode, with calibration performed with the ION-TOF measurement explorer software (Version 6.3).

The deposition and XPS characterization were performed at the University of California, Riverside, and then the samples were shipped to the University of Delaware for ToF-SIMS analysis, the same as in our previous work.[34] Measurements had been done three times for each sample. There are no noticeable changes among them, consistent with previous results that showed that if the samples are kept under nitrogen during shipping and installed immediately into the vacuum chamber of the ToF-SIMS instrument upon arrival, reliable information can be obtained about the surface species. We have also previously shown that the spectra of the adsorbates obtained by exposure of silica surfaces to the platinum precursor are not affected substantially upon being kept under nitrogen in the University of Delaware for several days.[34]

Computational investigation of the metalorganic compounds used for comparison with the chemistry of several ligands attached to platinum or nickel were performed with density functional theory (DFT) calculations using the Gaussian 09 suite of programs,[56] utilizing the B3LYP functional and the DEF2-TZVP basis set.[57−60] The calculations for the adsorption on a NiO(001) surface were carried out using the projector augmented wave (PAW) method and DFT as implemented in the VASP code.[61,62] To describe the electronic structure of NiO we used a Hubbard-*U* correction in the form of DFT+*U*[63,64] with $U-J$ = 5 eV, based on previous work,[65,66] and a cutoff energy of 415 eV for the plane-wave basis set. NiO crystallizes in rock salt structure with *Fm*3*m* space group.[67,68] The calculated equilibrium bulk lattice parameter of 4.155 Å is in good agreement with the experimental value of 4.176 Å.[69] For the surface calculations, we constructed a nonpolar NiO(001) slab consisting of eight atomic layers and a vacuum layer of 15 Å, and 4 × 4 in-plane unit cells to minimize interactions of the adsorbate species with their image in neighboring cells. We employed a 2 × 2 × 1 Monkhorst−Pack *k* mesh for integration over the Brillouin zone. The nonpolar NiO(001) surface exhibits the lowest surface energy of all planes of that oxide.[70] For structural relaxation, all the atomic positions were fully relaxed until the Hellman−Feynman force on each atom was less than 1×10^{-4} eV/Å. Finally, all calculations included spin-polarization due to the antiferromagnetic ground state of NiO.[67]

■ ASSOCIATED CONTENT

Supporting Information

This material is available free of charge at The Supporting Information is available free of charge at https://pubs.acs.org/doi/10.1021/acs.organomet.9b00781.

Computational model data (XYZ)

AFM images and coordinates of the structures used in Table 1 (PDF)

■ AUTHOR INFORMATION

Corresponding Author

Andrew V. Teplyakov − *Department of Chemistry and Biochemistry, University of Delaware, Newark, Delaware 19716, United States;* orcid.org/0000-0002-6646-3310; Phone: (302) 831-1969; Email: andrewt@udel.edu; Fax: (302) 831-6335

Authors

Mahsa Konh − *Department of Chemistry and Biochemistry, University of Delaware, Newark, Delaware 19716, United States*

Clinton Lien − *Department of Chemistry, University of California, Riverside, California 92521, United States*

Xuefen Cai − *Material Science and Engineering Department, University of Delaware, Newark, Delaware 19716, United States; Beijing Computational Science Research Center, Beijing 100193*

Su-Huai Wei − *Beijing Computational Science Research Center, Beijing 100193;* orcid.org/0000-0003-1563-4738

Anderson Janotti − *Material Science and Engineering Department, University of Delaware, Newark, Delaware 19716, United States*

Francisco Zaera − *Department of Chemistry, University of California, Riverside, California 92521, United States;* orcid.org/0000-0002-0128-7221

Complete contact information is available at: https://pubs.acs.org/10.1021/acs.organomet.9b00781

Notes

The authors declare no competing financial interest.

■ ACKNOWLEDGMENTS

The ToF-SIMS work at Delaware (AVT) was partially supported by the National Science Foundation (DMR1609973 (GOALI)) and by the University of Delaware. The synthesis and initial characterization of the samples in Riverside (FZ) was financed by a grant from the U.S. Department of Energy, Office of Science, Basic Energy Sciences, Materials Sciences and Engineering (MSE) Division, under Award No. DE-SC0001839. The authors also acknowledge the NSF (9724307; 1428149) and the NIH NIGMS COBRE program (P30-GM110758) for partial support of activities in the University of Delaware Surface Analysis Facility. AJ acknowledges support from NSF Faculty Early Career Development Program No. DMR-1652994, and XSEDE under National Science Foundation Grant No. ACI-1053575. XC and SHW acknowledge the support from the National Nature Science Foundation of China (No. 51672023; 11634003; U1930402) and computational support from the Beijing Computational Science Research Center (CSRC), and support from the China Scholarship Council (No. 201904890014). We also want to thank Mr. Chuan He (University of Delaware) and Dr. Taha Salavati-fard (University of Houston) for useful discussions.

■ REFERENCES

(1) Yang, H.; Coutanceau, C.; Léger, J. M.; Alonso-Vante, N.; Lamy, C. Methanol Tolerant Oxygen Reduction on Carbon-Supported Pt-Ni Alloy Nanoparticles. *J. Electroanal. Chem.* **2005**, *576* (2), 305−313.

(2) Lu, S.; Li, H.; Sun, J.; Zhuang, Z. Promoting the Methanol Oxidation Catalytic Activity by Introducing Surface Nickel on Platinum Nanoparticles. *Nano Res.* **2018**, *11* (4), 2058−2068.

(3) Jahan, M.; Liu, Z.; Loh, K. P. A Graphene Oxide and Copper-Centered Metal Organic Framework Composite as a Tri-Functional Catalyst for HER, OER, and ORR. *Adv. Funct. Mater.* **2013**, *23* (43), 5363−5372.

(4) Cornils, B.; Herrmann, W. A. *Applied Homogeneous Catalysis with Organometallic Compounds: A Comprehensive Handbook in Two Volumes*; Weinheim-VCH: New York, 1996.

(5) Schafer, L. L. Organometallics - A Foundation for Catalysis Research. *Organometallics* **2017**, *36* (11), 2053.

(6) Niu, Z.; Wang, D.; Yu, R.; Peng, Q.; Li, Y. Highly Branched Pt-Ni Nanocrystals Enclosed by Stepped Surface for Methanol Oxidation. *Chem. Sci.* **2012**, *3* (6), 1925−1929.

(7) Cao, Z.; Chen, Q.; Zhang, J.; Li, H.; Jiang, Y.; Shen, S.; Fu, G.; Lu, B. A.; Xie, Z.; Zheng, L. Platinum-Nickel Alloy Excavated Nano-Multipods with Hexagonal Close-Packed Structure and Superior

Activity towards Hydrogen Evolution Reaction. *Nat. Commun.* **2017**, *8*, 15131.
(8) Jiang, Q.; Jiang, L.; Wang, S.; Qi, J.; Sun, G. A Highly Active PtNi/C Electrocatalyst for Methanol Electro-Oxidation in Alkaline Media. *Catal. Commun.* **2010**, *12* (1), 67−70.
(9) Koponen, S. E.; Gordon, P. G.; Barry, S. T. Principles of Precursor Design for Vapour Deposition Methods. *Polyhedron* **2016**, *108*, 59.
(10) Mackus, A. J. M.; Verheijen, M. A.; Leick, N.; Bol, A. A.; Kessels, W. M. M. Influence of Oxygen Exposure on the Nucleation of Platinum Atomic Layer Deposition: Consequences for Film Growth, Nanopatterning, and Nanoparticle Synthesis. *Chem. Mater.* **2013**, *25* (9), 1905−1911.
(11) Wang, C.; Hu, L.; Poeppelmeier, K.; Stair, P. C.; Marks, L. Nucleation and Growth Process of Atomic Layer Deposition Platinum Nanoparticles on Strontium Titanate Nanocuboids. *Nanotechnology* **2017**, *28* (18), 185704.
(12) Aaltonen, T.; Ritala, M.; Sajavaara, T.; Keinonen, J.; Leskelä, M. Atomic Layer Deposition of Platinum Thin Films. *Chem. Mater.* **2003**, *15* (9), 1924−1928.
(13) Camacho-Bunquin, J.; Ferrandon, M.; Sohn, H.; Yang, D.; Liu, C.; Ignacio-De Leon, P. A.; Perras, F. A.; Pruski, M.; Stair, P. C.; Delferro, M. Chemoselective Hydrogenation with Supported Organoplatinum(IV) Catalyst on Zn(II)-Modified Silica. *J. Am. Chem. Soc.* **2018**, *140* (11), 3940−3951.
(14) George, S. M. Atomic Layer Deposition: An Overview. *Chem. Rev.* **2010**, *110* (1), 111−131.
(15) Leskelä, M.; Niinistö, J.; Ritala, M. Atomic Layer Deposition. In *Comprehensive Materials Processing*; Elsevier: Oxford, 2014; pp 101−123.
(16) Lien, C.; Konh, M.; Chen, B.; Teplyakov, A. V.; Zaera, F. Gas-Phase Electron-Impact Activation of Atomic Layer Deposition (ALD) Precursors: $MeCpPtMe_3$. *J. Phys. Chem. Lett.* **2018**, *9* (16), 4602−4606.
(17) Joo, J. B.; Dillon, R.; Lee, I.; Yin, Y.; Bardeen, C. J.; Zaera, F. Promotion of Atomic Hydrogen Recombination as an Alternative to Electron Trapping for the Role of Metals in the Photocatalytic Production of H_2. *Proc. Natl. Acad. Sci. U. S. A.* **2014**, *111* (22), 7942−7947.
(18) Luna, A. L.; Novoseltceva, E.; Louarn, E.; Beaunier, P.; Kowalska, E.; Ohtani, B.; Valenzuela, M. A.; Remita, H.; Colbeau-Justin, C. Synergetic Effect of Ni and Au Nanoparticles Synthesized on Titania Particles for Efficient Photocatalytic Hydrogen Production. *Appl. Catal., B* **2016**, *191*, 18−28.
(19) Clancey, J. W.; Cavanagh, A. S.; Kukreja, R. S.; Kongkanand, A.; George, S. M. Atomic Layer Deposition of Ultrathin Platinum Films on Tungsten Atomic Layer Deposition Adhesion Layers: Application to High Surface Area Substrates. *J. Vac. Sci. Technol., A* **2015**, *33* (1), 01A130.
(20) Lee, H. B. R.; Bent, S. F. Formation of Continuous Pt Films on the Graphite Surface by Atomic Layer Deposition with Reactive O_3. *Chem. Mater.* **2015**, *27* (19), 6802−6809.
(21) Lien, C.; Sun, H.; Qin, X.; Zaera, F. Platinum Atomic Layer Deposition on Metal Substrates: A Surface Chemistry Study. *Surf. Sci.* **2018**, *677* (July), 161−166.
(22) Xue, Z.; Kaesz, H. D.; Thridandam, H.; Hicks, R. F. Organometallic Chemical Vapor Deposition of Platinum. Reaction Kinetics and Vapor Pressures of Precursors. *Chem. Mater.* **1992**, *4* (1), 162−166.
(23) Aaltonen, T.; Ritala, M.; Sajavaara, T.; Keinonen, J.; Leskelä, M. Atomic Layer Deposition of Platinum Thin Films. *Chem. Mater.* **2003**, *15* (9), 1924−1928.
(24) Mackus, A. J. M.; Leick, N.; Baker, L.; Kessels, W. M. M. Catalytic Combustion and Dehydrogenation Reactions during Atomic Layer Deposition of Platinum. *Chem. Mater.* **2012**, *24* (10), 1752−1761.
(25) Lubers, A. M.; Muhich, C. L.; Anderson, K. M.; Weimer, A. W. Mechanistic Studies for Depositing Highly Dispersed Pt Nanoparticles on Carbon by Use of Trimethyl(Methylcyclopentadienyl)-Platinum(IV) Reactions with O_2 and H_2. *J. Nanopart. Res.* **2015**, *17*, 179.
(26) Bosch, R. H. E. C.; Bloksma, F. L.; Huijs, J. M. M.; Verheijen, M. A.; Kessels, W. M. M. Surface Infrared Spectroscopy during Low Temperature Growth of Supported Pt Nanoparticles by Atomic Layer Deposition. *J. Phys. Chem. C* **2016**, *120* (1), 750−755.
(27) Erkens, I. J. M.; Mackus, A. J. M.; Knoops, H. C. M.; Smits, P.; Van De Ven, T. H. M.; Roozeboom, F.; Kessels, W. M. M. Mass Spectrometry Study of the Temperature Dependence of Pt Film Growth by Atomic Layer Deposition. *ECS J. Solid State Sci. Technol.* **2012**, *1* (6), P255.
(28) Kessels, W. M. M.; Knoops, H. C. M.; Dielissen, S. A. F.; Mackus, A. J. M.; Van De Sanden, M. C. M. Surface Reactions during Atomic Layer Deposition of Pt Derived from Gas Phase Infrared Spectroscopy. *Appl. Phys. Lett.* **2009**, *95* (1), 1−4.
(29) Diskus, M.; Balasundaram, M.; Nilsen, O.; Fjellvåg, H. Influence of Precursors Chemistry on ALD Growth of Cobalt-Molybdenum Oxide Films. *Dalt. Trans.* **2012**, *41* (8), 2439−2444.
(30) Elam, J. W.; Pellin, M. J.; Elliott, S. D.; Zydor, A.; Faia, M. C.; Hupp, J. T. Mechanism for Zirconium Oxide Atomic Layer Deposition Using Bis(Methylcyclopentadienyl)Methoxymethyl Zirconium. *Appl. Phys. Lett.* **2007**, *91* (25), 253123.
(31) Bouman, M.; Zaera, F. Kinetics of Adsorption of Methylcyclopentadienyl Manganese Tricarbonyl on Copper Surfaces and Implications for the Atomic Layer Deposition of Thin Solid Films. *J. Phys. Chem. C* **2016**, *120* (15), 8232−8239.
(32) Bouman, M.; Qin, X.; Doan, V.; Groven, B. L. D.; Zaera, F. Reaction of Methylcyclopentadienyl Manganese Tricarbonyl on Silicon Oxide Surfaces: Implications for Thin Film Atomic Layer Depositions. *Organometallics* **2014**, *33* (19), 5308−5315.
(33) Aaltonen, T.; Rahtu, A.; Ritala, M.; Leskelä, M. Reaction Mechanism Studies on Atomic Layer Deposition of Puthenium and Platinum. *Electrochem. Solid-State Lett.* **2003**, *6* (9), C130.
(34) Konh, M.; Lien, C.; Zaera, F.; Teplyakov, A. V. Application of Time-of-Flight Secondary Ion Mass Spectrometry to the Detection of Surface Intermediates during the First Cycle of Atomic Layer Deposition (ALD) of Platinum on Silica Surfaces. *Appl. Surf. Sci.* **2019**, *488*, 468−476.
(35) Engmann, S.; Stano, M.; Matejík, T.; Ingólfsson, O. Electron Induced Reactions in Gas Phase $MeCpPtMe_3$ and $Pd(Hfac)_2$. *J. Phys.: Conf. Ser.* **2012**, *388* (5), 4−5.
(36) Baryshev, S. V.; Zinovev, A. V.; Tripa, C. E.; Pellin, M. J.; Peng, Q.; Elam, J. W.; Veryovkin, I. V. High-Resolution Secondary Ion Mass Spectrometry Depth Profiling of Nanolayers. *Rapid Commun. Mass Spectrom.* **2012**, *26* (19), 2224−2230.
(37) Vanfleet, R.; Linford, M.; Davis, R.; Jensen, D.; Kanyal, S.; Dadson, A. Atomic Layer Deposition of Aluminum-Free Silica onto Patterned Carbon Nanotube Forests in the Preparation of Microfabricated Thin-Layer Chromatography Plates. *J. Planar Chromatogr.–Mod. TLC* **2014**, *27* (3), 151−156.
(38) Terlier, T.; Maindron, T.; Barnes, J. P.; Léonard, D. Characterization of Advanced ALD-Based Thin Film Barriers for Organic Electronics Using ToF-SIMS Analysis. *Org. Electron.* **2018**, *59* (April), 21−26.
(39) Ni, C.; Zhang, Z.; Wells, M.; Beebe, T. P., Jr.; Pirolli, L.; Méndez De Leo, L. P.; Teplyakov, A. V. Effect of Film Thickness and the Presence of Surface Fluorine on the Structure of a Thin Barrier Film Deposited from Tetrakis-(Dimethylamino)-Titanium onto a Si(100)-2 × 1 Substrate. *Thin Solid Films* **2007**, *515* (5), 3030−3039.
(40) Bocharov, S.; Zhang, Z.; Beebe, T. P., Jr.; Teplyakov, A. V. Structure of a Thin Barrier Film Deposited from Tetrakis-(Dimemylamino)-Titanium onto a Si(100)-2 × 1 Substrate. *Thin Solid Films* **2005**, *471* (1−2), 159−165.
(41) Wagner, C. D.; Riggs, W. M.; Davis, L. E.; Moulder, J. F.; Muilenberg, G. E. *Handbook of X-Ray Photoelectron Spectroscopy*; Perkin-Elmer Corporation: Eden Prairie, MN, 1978.
(42) Mackus, A. J. M.; Garcia-Alonso, D.; Knoops, H. C. M.; Bol, A. A.; Kessels, W. M. M. Room-Temperature Atomic Layer Deposition of Platinum. *Chem. Mater.* **2013**, *25* (9), 1769−1774.

https://dx.doi.org/10.1021/acs.organomet.9b00781
Organometallics 2020, 39, 1024−1034

(43) Collman, J. P.; Hegedus, L. G.; Norton, J. R.; Finke, R. G. *Principles and Applications of Organotransition Metal Chemistry*; Oxford University Press: Oxford, UK, 1987.
(44) Zaera, F. Study of the Surface Chemistry of Methyl Iodide Coadsorbed with Hydrogen on Pt(111). *Surf. Sci.* **1992**, *262* (3), 335−350.
(45) Tjandra, S.; Zaera, F. Methyl Iodide Thermal Reactions When Chemisorbed on Ni(100) Surfaces. *Langmuir* **1992**, *8* (9), 2090−2097.
(46) Gleason, N. R.; Zaera, F. The Use of Low-Energy Ion Scattering Spectroscopy for the Quantitative Determination of Adsorption Sites in Surface Chemistry Studies. *Surf. Sci.* **1997**, *385* (2−3), 294−309.
(47) Zaera, F. An Organometallic Guide to the Chemistry of Hydrocarbon Moieties on Transition Metal Surfaces. *Chem. Rev.* **1995**, *95* (8), 2651−2693.
(48) Bent, B. E. Mimicking Aspects of Heterogeneous Catalysis: Generating, Isolating, and Reacting Proposed Surface Intermediates on Single Crystals in Vacuum. *Chem. Rev.* **1996**, *96* (4), 1361−1390.
(49) Siegbahn, P. E.M.; Panas, I. A Theoretical Study of CH_x, Chemisorption on the Ni(100) and Ni(111) Surfaces. *Surf. Sci.* **1990**, *240*, 37−49.
(50) Kua, J.; Goddard, W. A. Chemisorption of Organics on Platinum. 2. Chemisorption of C_2H_x and CH_x on Pt(111). *J. Phys. Chem. B* **1998**, *102* (47), 9492−9500.
(51) Comelli, N. C.; López, M. B.; Castro, E. A. Theoretical Study of the Adsorption of C_5H_n (N = 5,8,10) on Ni(100) and Ni(111) Surfaces. *J. Mol. Struct.: THEOCHEM* **2005**, *726* (1−3), 197−204.
(52) Brizuela, G.; Castellani, N. J. C_5H_n Rings Adsorbed on Pt(111): A Theoretical Study. *Surf. Sci.* **1998**, *401* (3), 297−311.
(53) Tiznado, H.; Zaera, F. Surface Chemistry in the Atomic Layer Deposition of TiN Films from $TiCl_4$ and Ammonia. *J. Phys. Chem. B* **2006**, *110* (27), 13491−13498.
(54) Sun, H.; Zaera, F. Chemical Vapor Deposition of Manganese Metallic Films on Silicon Oxide Substrates. *J. Phys. Chem. C* **2012**, *116* (44), 23585−23595.
(55) Sun, H.; Qin, X.; Zaera, F. Activation of Metal-Organic Precursors by Electron Bombardment in the Gas Phase for Enhanced Deposition of Solid Films. *J. Phys. Chem. Lett.* **2012**, *3* (17), 2523−2527.
(56) Frisch, M. J.; Trucks, G. W.; Schlegel, H. B.; Scuseria, G. E.; Robb, M. A.; Cheeseman, J. R.; Scalmani, G.; Barone, V.; Mennucci, B.; Petersson, G. A.; Nakatsuji, H.; Caricato, M.; Li, X.; Hratchian, H. P.; Izmaylov, A. F.; Bloino, J.; Zheng, G.; Sonnenberg, J. L.; Hada, M.; Ehara, M.; Toyota, K.; Fukuda, R.; Hasegawa, J.; Ishida, M.; Nakajima, T.; Honda, Y.; Kitao, O.; Nakai, H.; Vreven, T.; Montgomery, J. A., Jr.; Peralta, J. E.; Ogliaro, F.; Bearpark, M.; Heyd, J. J.; Brothers, E.; Kudin, K. N.; Staroverov, V. N.; Kobayashi, R.; Normand, J.; Raghavachari, K.; Rendell, A.; Burant, J. C.; Iyengar, S. S.; Tomasi, J.; Cossi, M.; Rega, N.; Millam, N. J.; Klene, M.; Knox, J. E.; Cross, J. B.; Bakken, V.; Adamo, C.; Jaramillo, J.; Gomperts, R.; Stratmann, R. E.; Yazyev, O.; Austin, A. J.; Cammi, R.; Pomelli, C.; Ochterski, J. W.; Martin, R. L.; Morokuma, K.; Zakrzewski, V. G.; Voth, G. A.; Salvador, P.; Dannenberg, J. J.; Dapprich, S.; Daniels, A. D.; Farkas, Ö.; Foresman, J. B.; Ortiz, J. V.; Cioslowski, J.; Fox, D. J. *Gaussian 09*, Revision B.01.; Gaussian, Inc.: Wallingford, CT, 2009.
(57) Schäfer, A.; Horn, H.; Ahlrichs, R. Fully Optimized Contracted Gaussian Basis Sets for Atoms Li to Kr. *J. Chem. Phys.* **1992**, *97* (4), 2571−2577.
(58) Weigend, F.; Ahlrichs, R. Balanced Basis Sets of Split Valence, Triple Zeta Valence and Quadruple Zeta Valence Quality for H to Rn: Design and Assessment of Accuracy. *Phys. Chem. Chem. Phys.* **2005**, *7* (18), 3297−3305.
(59) Weigend, F. Accurate Coulomb-Fitting Basis Sets for H to Rn. *Phys. Chem. Chem. Phys.* **2006**, *8* (9), 1057−1065.
(60) Schäfer, A.; Huber, C.; Ahlrichs, R. Fully Optimized Contracted Gaussian Basis Sets of Triple Zeta Valence Quality for Atoms Li to Kr. *J. Chem. Phys.* **1994**, *100* (8), 5829−5835.
(61) Kresse, G.; Joubert, D. From Ultrasoft Pseudopotentials to the Projector Augmented-Wave Method. *Phys. Rev. B: Condens. Matter Mater. Phys.* **1999**, *59* (3), 1758−1775.
(62) Kresse, G.; Furthmüller, J. Efficient Iterative Schemes for Ab Initio Total-Energy Calculations Using a Plane-Wave Basis Set. *Phys. Rev. B: Condens. Matter Mater. Phys.* **1996**, *54* (16), 11169−11186.
(63) Anisimov, V. I.; Aryasetiawan, F.; Lichtenstein, A. I. First-Principles Calculations of the Electronic Structure and Spectra of Strongly Correlated Systems: The LDA + U Method. *J. Phys.: Condens. Matter* **1997**, *9* (4), 767−808.
(64) Anisimov, V. I.; Zaanen, J.; Andersen, O. K. Band Theory and Mott Insulators: Hubbard U Instead of Stoner I. *Phys. Rev. B: Condens. Matter Mater. Phys.* **1991**, *44* (3), 943−954.
(65) Rohrbach, G.; Hafner, J.; Kresse, G. Molecular Adsorption on the Surface of Strongly Correlated Transition-Metal Oxides: A Case Study for CO/NiO(100). *Phys. Rev. B: Condens. Matter Mater. Phys.* **2004**, *69* (7), 1−13.
(66) Li, L.; Kanai, Y. Antiferromagnetic Structures and Electronic Energy Levels at Reconstructed NiO(111) Surfaces: A DFT+U Study. *Phys. Rev. B: Condens. Matter Mater. Phys.* **2015**, *91* (23), 1−10.
(67) Smart, J. S.; Greenwald, S. Crystal Structure Transitions in Antiferromagnetic Compounds at the Curie Temperature. *Phys. Rev.* **1951**, *82*, 113−114.
(68) Tombs, N. C.; Rooksby, H. P. Structure of Monoxides of Some Transition Elements at Low Temperatures. *Nature* **1950**, *165*, 442−443.
(69) Ohldag, H.; Van Der Laan, G.; Arenholz, E. Correlation of Crystallographic and Magnetic Domains at Co/NiO(001) Interfaces. *Phys. Rev. B: Condens. Matter Mater. Phys.* **2009**, *79* (5), 2−5.
(70) Tasker, P. W.; Duffy, D. M. The Structure and Properties of the Stepped Surfaces of MgO and NiO. *Surf. Sci.* **1984**, *137* (1), 91−102.

https://dx.doi.org/10.1021/acs.organomet.9b00781
Organometallics 2020, 39, 1024−1034